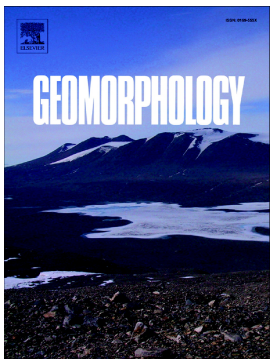

Sulfur and oxygen isotopes in the gypsum deposits of the Provalata sulfuric acid cave (Macedonia)

Marjan Temovski, István Futó, Marianna Túri, László Palcsu

PII: S0169-555X(18)30203-4
DOI: doi:10.1016/j.geomorph.2018.05.010
Reference: GEOMOR 6397

To appear in: *Geomorphology*

Received date: 11 October 2017
Revised date: 7 May 2018
Accepted date: 12 May 2018

Please cite this article as: Marjan Temovski, István Futó, Marianna Túri, László Palcsu , Sulfur and oxygen isotopes in the gypsum deposits of the Provalata sulfuric acid cave (Macedonia). The address for the corresponding author was captured as affiliation for all authors. Please check if appropriate. Geomor(2017), doi:10.1016/j.geomorph.2018.05.010

Sulfur and oxygen isotopes in the gypsum deposits of the Provalata sulfuric acid cave (Macedonia)

Marjan Temovski[1]*, István Futó[2], Marianna Túri[3], László Palcsu[4]

Isotope Climatology and Environmental Research Centre, Institute for Nuclear Research, Hungarian Academy of Sciences, Bem tér 18/c, 4026, Debrecen, Hungary

*Corresponding author

E-mail addresses:

[1] temovski.marjan@atomki.mta.hu, [2] futo.istvan@atomki.mta.hu,

[3] turi.marianna@atomki.mta.hu, [4] palcsu.laszlo@atomki.mta.hu

Highlights

- Use of both $\delta^{18}O$ and $\delta^{34}S$ in the study of gypsum deposits from a sulfuric acid cave
- Positive correlation between $\delta^{18}O$ and $\delta^{34}S$ due to both oxygen and sulfur isotopes being concurrently affected during H_2S oxidation
- Evolution of the sulfur stable isotopes in the H_2S of the sulfuric acid speleogenesis

Abstract

Sulfur stable isotopes from cave sulfates (mainly gypsum) have been used in a number of studies to trace the source of sulfur in caves formed by sulfuric acid, but only few studies apply combined use of sulfur and oxygen stable isotopes to further understand the processes operating in sulfuric acid speleogenesis (SAS). Here we present results of a detailed study of

the distribution of sulfur and oxygen stable isotopes within the gypsum deposits formed during sulfuric acid speleogenesis of Provalata Cave (Macedonia). The $\delta^{18}O$ (vs VSMOW) values range between -3.9 ‰ and +8.2 ‰, and the $\delta^{34}S$ (vs CDT) values between -7.5 ‰ and +0.7 ‰. We found a strong positive correlation between the $\delta^{18}O$ and $\delta^{34}S$ values, with a 0.5 ‰ increase in the $\delta^{34}S$ for every 1 ‰ increase in the $\delta^{18}O$, indicating that both oxygen and sulfur isotopes were concurrently affected during the oxidation process. We attribute these effects to be either due to environmental control (concentrations of H_2S and O_2) or due to isotope fractionation during multi-step microbial oxidation, also affected by the environmental conditions. Additionally a shift of +1.85 ‰ in the $\delta^{34}S$ values prior to the H_2S oxidation is found, indicating evolution of the H_2S $\delta^{34}S$ in the SAS system. The wide range of both $\delta^{18}O$ and $\delta^{34}S$ values in the gypsum deposits of the small Provalata Cave show that both the number of samples and their location can be an important factor for the understanding of sulfuric acid speleogenesis using stable isotopes.

Keywords:

Gypsum; sulfur isotopes; oxygen isotopes; sulfuric acid cave; speleogenesis; Provalata Cave

1. Introduction

Sulfuric acid caves are an important genetic subgroup of hypogene caves, developed due to dissolution of carbonate rocks (limestone, dolomite, marble) by sulfuric acid (sulfuric acid speleogenesis; SAS), which forms as a result of oxidation of sulfides (typically H_2S) at or near the water table (Palmer, 2013). These caves share common morphological features (Hill, 1987; Audra et al., 2007; Plan et al., 2012; Palmer, 2013; De Waele et al., 2016), as well as

secondary sulfate minerals, with gypsum (formed at the contact of sulfuric acid and carbonate rocks) as the most typical one (Galdenzi and Maruoka, 2003).

Although H_2S oxidation (abiotic or biotic) and sulfuric acid dissolution can happen both above and below the water table (Egemeier, 1981; Hill, 1987; Engel et al., 2004; Galdenzi et al., 2008), most of the cave volume development is considered to be subaerial by condensation corrosion (Palmer, 2013; De Waele et al., 2016). A recent study by Jones et al. (2015) on the example of Frassasi Caves showed that H_2S degassing is much more important in turbulent, flowing waters compared to stagnant pools, even in the presence of abundant sulfide-oxidizing microbiota, suggesting that in such a situation, subaerial SAS is much more important than subaqueous SAS. In such settings, H_2S oxidizes to sulfuric acid on moist cave walls and ceilings, dissolving limestone and precipitating gypsum as gypsum replacement crusts (Galdenzi and Maruoka, 2003; Palmer, 2013; Piccini et al., 2015).

A frequent question in the study of SAS caves has been the source of sulfur, with sulfur isotope composition ($\delta^{34}S$) of SAS products typically used to identify the source in a number of studies (e.g. Hill, 1987; Bottrell, 1991; Bottrell et al., 2001; Galdenzi and Maruoka, 2003; Wynn et al., 2010). The $\delta^{18}O$ of SAS sulfate products on the other hand is less commonly studied, with only few publications found (e.g. Van Everdingen et al., 1985; Grasby et al., 2003; Onac et al., 2011). In a recent study of the sulfate minerals (mainly gypsum) deposited in a variety of cave settings in Cerna Valley (Romania), Onac et al. (2011) showed that the combined use of oxygen and sulfur stable isotopes can provide more complete insight into the range of processes operating in SAS. In their study, they defined three distinct populations of sulfate minerals, and demonstrate the variation of the sulfur and oxygen stable isotope signatures in a wider (regional) sense.

Here we present a detailed study of the sulfur and oxygen stable isotopes in the gypsum deposits of Provalata Cave (Macedonia), showing local (within cave) variation of their values, and discuss possible implications for the interpretation of SAS processes based on oxygen and sulfur isotopes in the sulfate deposits.

2. Sources and fractionation of sulfur and oxygen isotopes in sulfuric acid speleogenesis

In the SAS, gypsum ($CaSO_4 \cdot 2H_2O$) forms as a result of the reaction between sulfuric acid (H_2SO_4) and the carbonate bedrock, with CO_2 as a by-product. Sulfuric acid forms as a result of oxidation of sulfides, predominantly hydrogen sulfide (H_2S) (Palmer, 1991). Oxidation of pyrite (FeS_2) found within the carbonate rocks, or adjacent non-carbonate sediments, can also produce sulfuric acid but this mechanism is considered as speleogenetically less significant (Palmer, 1991), although it can contribute even if the dominant source is H_2S (e.g. Onac et al., 2011). For most of the SAS caves, the source of H_2S has been attributed to microbial reduction of sulfates, with hydrocarbons serving as electron donors (Hill, 1987; Hose et al., 2000; Onac et al., 2011).

The $\delta^{34}S$ value of the sulfur in the speleogenetic gypsum depends on the pathways and processes which have occurred along the way, from the production of H_2S, through oxidation to sulfuric acid, and deposition of gypsum. The original $\delta^{34}S$ of the source H_2S, if being produced by microbially mediated reduction of sulfates, depends on: the original sulfate $\delta^{34}S$ values, the fractionation occurring during the reduction as well as the completeness of the process, with complete reduction reflecting original $\delta^{34}S$ of the sulfate, and partial reduction having much more negative values (Wynn et al., 2010). The morphology and deposits related to SAS in Provalata Cave suggest dissolution by sulfuric acid due to H_2S oxidation mostly

above the water table (Temovski et al., 2013). As we cannot say much about the source of the H_2S in the Provalata Cave, with nearby coal deposits considered as a possibility (Temovski et al., 2013), we will briefly review the processes and possible changes of the sulfur isotope values from when the $H_2S_{(aq)}$ reached the cave, through its oxidation and sulfate deposition as gypsum.

Within the hypogene cave system, the oxidation of H_2S can happen near or at the water table, where oxygen-rich vadose waters reach the water table, or above by reaction with condensation water. Near or at the water table, H_2S can oxidize to sulfuric acid (via intermediate sulfur species) either abiotically or microbially, the latter being found as much more important (Engel et al., 2004; Jones et al., 2015). During abiotic oxidation by O_2, the produced sulfate is depleted in ^{34}S, with fractionation of ~-5 ‰ (Fry et al., 1988). For chemolithotrophic oxidation of H_2S to S^0, on the example of Frasassi Caves, fractionation from -0.3 to +8 ‰ was calculated. This is greater than estimations from previous laboratory studies, with isotope fractionation of S^0 after complete oxidation to SO_4 considered to be very small to negligible (Zerkle et al., 2016 and references therein).

The $\delta^{34}S$ of the dissolved sulfate in the water, and the gypsum that can precipitate from it, can be affected also by additional sulfate introduced from the aerated zone, as well as by H_2S production by local microbial reduction of the dissolved sulfate. In Frasassi Cave, while microbial oxidation of H_2S has been detected in the groundwater, the groundwater was still found to be undersaturated with gypsum. Further, with gypsum depositing above the water table, it was proposed that H_2S oxidation above the water table and dissolution by condensation water was responsible for the formation of gypsum (Galdenzi and Maruoka, 2003).

Sulfur isotopes can also be fractionated during H_2S degassing. Depending on the pH of the groundwater, the $\delta^{34}S$ of $H_2S_{(g)}$ can become lower (by -0.9 ‰) at low pH. This effect decreases and becomes inverse near neutral pH, turning to higher values (up to +2.9 ‰) at high pH (Baune and Böttcher, 2010).

Within the cave atmosphere, the escaped H_2S can oxidize to sulfuric acid on cave walls, and condensation-corrosion by sulfuric acid will dissolve the carbonate rock, precipitating gypsum as replacement crusts (Galdenzi and Maruoka, 2003; Palmer, 2013). Some of the H_2S can escape the cave, especially in more aerated passages, which can lead to partial oxidation of the H_2S and sulfuric acid with more positive $\delta^{34}S$ values. Mansor et al. (2016) reported that $\delta^{34}S$ values of both H_2S and associated gypsum deposits decreased with height, indicating that diffusive fractionation of H_2S can contribute to 6-8 ‰ fractionation in gypsum over two meters distance. Another factor affecting the $\delta^{34}S$ values during H_2S oxidation can be the ratio of H_2S/O_2 concentration, with more than +4 ‰ higher $\delta^{34}S$ values found when higher O_2 and/or lower H_2S concentrations are encountered (Zerkle et al., 2016).

On the cave walls, oxidation of H_2S can be either abiotic or biotic, with the oxygen derived either from H_2O or O_2. The $\delta^{18}O$ value of the produced sulfate will depend on the fractions of oxygen derived from water or molecular oxygen and their isotope composition, as well as the oxygen enrichment factors between sulfate and H_2O ($\varepsilon^{18}_{SO4–H2O}$) and sulfate and O_2 ($\varepsilon^{18}_{SO4–O2}$). Both vary significantly but $\varepsilon^{18}_{SO4–H2O}$ is always positive (0 to +9.7 ‰) and $\varepsilon^{18}_{SO4–O2}$ is always negative (0 to -11.4 ‰) (Van Stempvoort and Krouse, 1994; Onac et al., 2011). Based on this the sulfate $\delta^{18}O$ values can be described as $\delta^{18}O_{SO4} = X * (\delta^{18}O_{H2O} + \varepsilon^{18}_{SO4–H2O}) + (1-X) * (\delta^{18}O_{O2} + \varepsilon^{18}_{SO4–O2})$, with X being the fraction of oxygen derived from water. However, this does not include the possible effects that can arise from exchange of oxygen isotopes between intermediate sulfur species (particularly S(IV) – sulfite/hydrogen sulfite) and water molecules (Van Stempvoort and Krouse, 1994).

During precipitation of gypsum there is also a small fractionation in both oxygen and sulfur isotopes. Oxygen in gypsum has been reported to be enriched by +2 ‰ to +3.6 ‰ (Lloyd, 1968) and +3.3 ‰ (Van Driessche et al., 2016), with smaller values reported for sulfur, between +1.1 ‰ and +2 ‰ (Thode and Monster, 1965; Raab and Spiro, 1991; Van Driessche et al., 2016).

3. The SAS of Provalata Cave

Provalata Cave is a small hypogene cave in Macedonia, located on the southern side of the Buturica Valley, with remnants of cave features found at the surface along the slope of the valley, and a small low-temperature (20–22 °C) thermal spring (Melnica Spring) located in the riverbed below the cave (Fig. 1). Provalata Cave has passages developed in marble during two geochemically different phases: the first due to cooling of CO_2-rich thermal waters, and the second due to sulfuric acid dissolution, separated by filling of passages with clay deposits (Temovski et al., 2013). Both phases are recognizable by distinct morphology and associated deposits, with phreatic morphologies covered by thick calcite coatings representative of the first phase, and vadose condensation-corrosion morphologies (feeders, half channels, pockets, cupolas), gypsum replacement crusts and other sulfate minerals (alunite, natroalunite, jarosite) formed as part of the second phase. Alunite and jarosite, which formed during the second phase, were Ar-Ar dated at ~1.5 Ma (Temovski et al., 2013). Preliminary sulfur isotope analysis from a sample of gypsum deposits gave values of -2.1 ‰ and -2.2 ‰ (Temovski et al., 2013). The cave is rich in gypsum deposits and, despite the old age of the SAS phase, they are quite well preserved, with intrusion of vadose waters notable only in a few locations where gypsum deposits have been mostly dissolved.

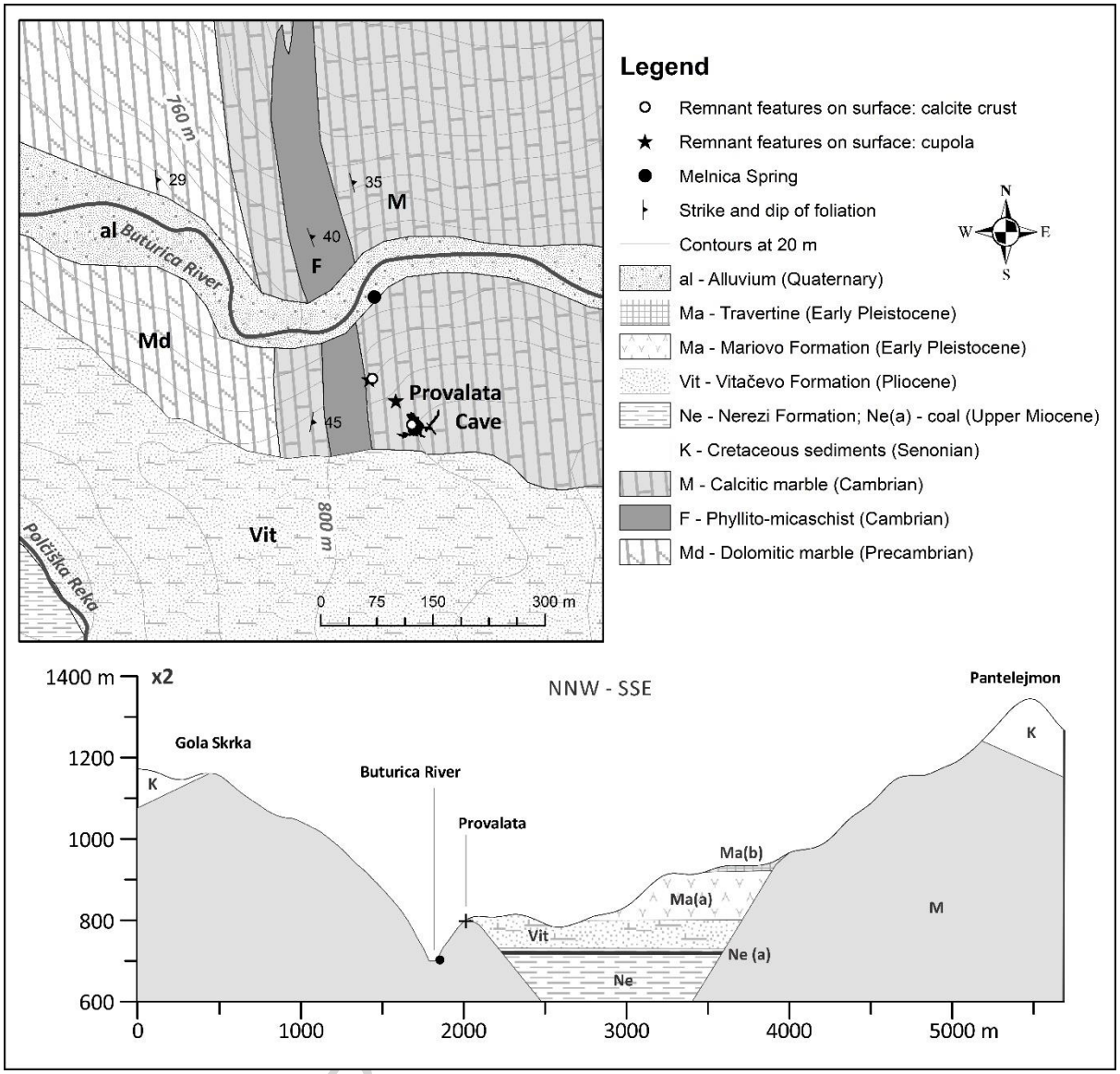

Fig. 1. Location and geological setting of Provalata Cave. Nerezi Formation is composed of clastic sediments and Vitačevo and Mariovo Formations of volcanoclastic sediments.

4. Methodology

Gypsum deposits in Provalata Cave were sampled at six locations: two samples were collected from both the Upper and Lower Passage, and one sample from both First and Second Room (Fig. 2). They were collected as cores drilled from detached replacement crusts, hand samples from replacement crusts, and from gypsum layers within floor

sediments. The drilling was performed using a 2.5 cm diameter corer, using the same approach applied to carbonate speleothems (Spötl and Mattey, 2012). Three of the samples, (G1, G2, and G6) were drilled from detachment crusts from the surface inwards, collecting partially complete cores with lengths of ~150 mm, ~100 mm, and ~80 mm (Figs. 3, 4). G4 was collected as hand sample from a (~50 mm thick) detached crust fallen on the floor. G5 was collected from slightly detached replacement crust with a thickness of ~80 mm and G3 was the only one that was sub-sampled directly, from gypsum layers within floor sediments (Figs. 3, 4). All of the gypsum samples are composed of finely crystalline white gypsum, recrystallized on the surface of the replacement crusts, with G5 having banding of more or less yellowish color, and G1 showing two yellowish bands, one near the surface and one in the middle (Fig. 4).

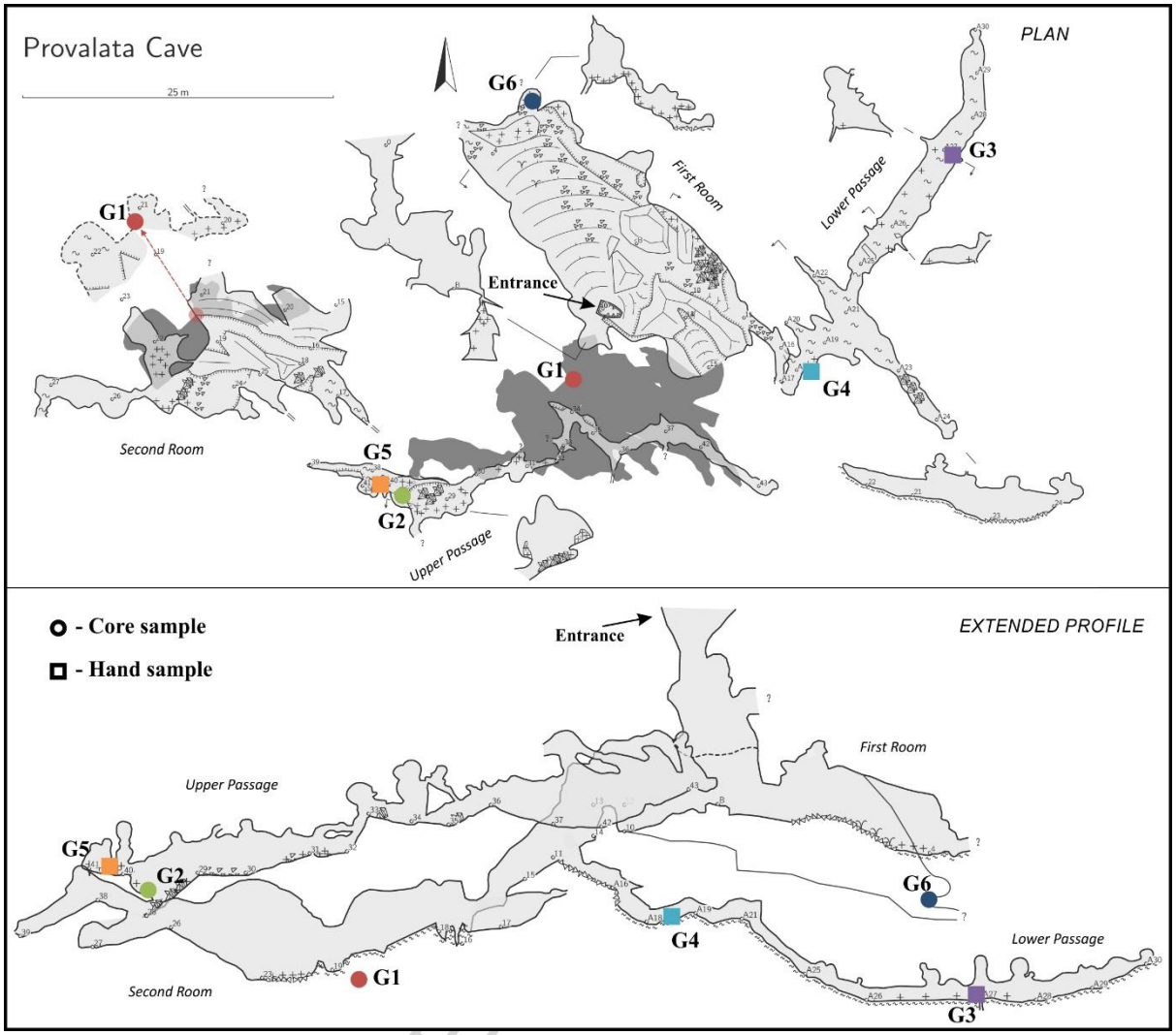

Fig. 2. Location and type of gypsum samples collected from Provalata Cave. This figure is available in color online at https://www.journals.elsevier.com/geomorphology.

Collected samples were cut, cleaned and left overnight to dry on room temperature, and ~4.5 mg sub-samples were collected from cores and hand samples at resolution of ~5 mm from a cut surface along a profile line. From sample G5, after the first sub-sampling (profile line/subset G5a) was performed on a coarser (break) profile surface, we made an additional sampling with a slightly higher resolution (profile line/subset G5b) from a newly cut profile surface (Fig. 4). To remove the gypsum hydration water and measure only the sulfate part, the sub-samples were dissolved in 2.5 M HCl and the sulfate ions were precipitated as $BaSO_4$. At four locations the sampled amount was ~10 mg, and half of the material was

separated for measurements of bulk gypsum stable isotope composition as a control on $\delta^{34}S$ during conversion from gypsum to barium sulfate ($BaSO_4$).

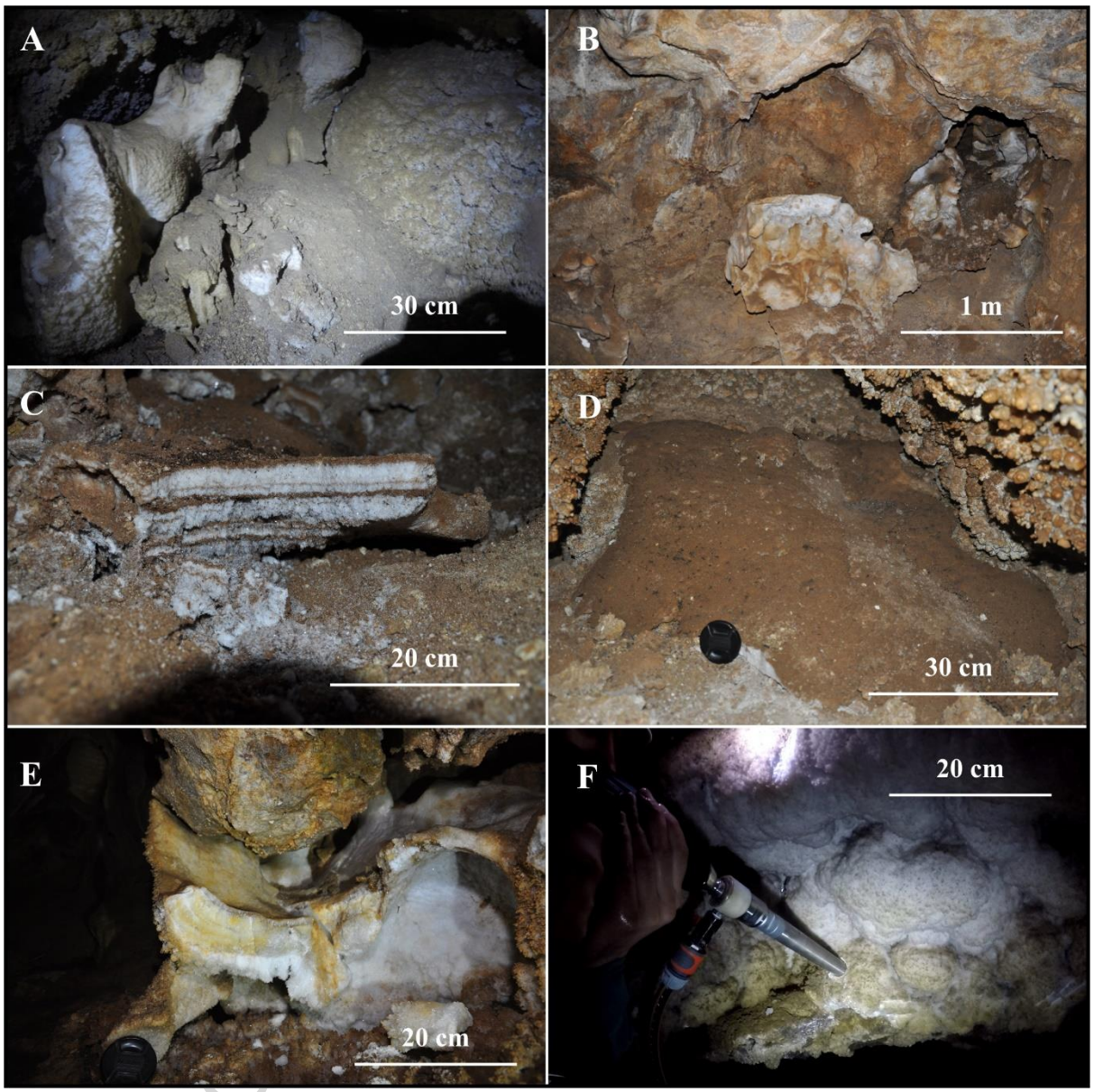

Fig. 3. Photos of sampling locations within the cave: A – Slightly detached gypsum replacement crust in a small side passage in Second Room (G1); B – Detached gypsum replacement crust close to the wall of a dome-like enlargement at the junction of passages in the Upper Passage (G2); C – Gypsum layers alternating with thin sandy layers on the foothill of the wall in the Lower Passage (G3); D – Gypsum crust covering the floor in the upper parts of the Lower Passage (G4); E - Slightly detached gypsum crust which was covering

calcite crust in a small dead-end part of the Upper Passage (G5); F – Gypsum replacement crust below a cupola carved in both calcite crust and bedrock in the northern end of the First Room (G6). Photos by M. Temovski. This figure is available in color online at https://www.journals.elsevier.com/geomorphology.

Sulfur and oxygen stable isotope ratios were measured at the Isotope Climatology and Environmental Research Centre (ICER), Institute for Nuclear Research (ATOMKI), Hungarian Academy of Sciences (MTA) by a Thermo Finnigan Delta^{PLUS} XP Isotope Ratio Mass Spectrometer using Thermal Combustion/Elemental Analyzer interface for the oxygen measurements and NA 1500 NCS Fisons Elemental Analyzer for the sulfur measurements. At least two of three standard materials (NBS-127, IAEA-SO-5 and IAEA-SO-6 for sulfur isotopes; NBS-127, IAEA-601 and IAEA-CH-3 for oxygen isotopes) were measured after the measurement of every 8 samples. The measured values are expressed in the delta notation as $\delta^{34}S$ and $\delta^{18}O$, with $\delta^{34}S$ given relative to CDT and $\delta^{18}O$ relative to VSMOW, where the delta values are defined as: δ (‰) = $(R_{sample}/ R_{reference}-1)*1000$, with R representing the $^{34}S/^{32}S$, $^{18}O/^{16}O$ ratio in the sample or in the international reference material. The precision of the stable isotope measurements, determined from replicate measurements of standard materials (total of 58 for sulfur and 63 for oxygen isotopes), is ±0.2 ‰ and ±0.5 ‰ or better for $\delta^{34}S$ and $\delta^{18}O$, respectively. A total of 123 sub-samples were measured, of which 105 were used for the statistical analyses, with values from subset G5a (N=18) excluded, as profile G5b has better sampling resolution than G5a.

Table 1. Results of test measurements for control of isotope changes during conversion of gypsum to barium sulfate.

Sample	$\delta^{34}S_{SO4}$	$\delta^{34}S_{gypsum(bulk)}$	$\delta^{18}O_{SO4}$	$\delta^{18}O_{gypsum(bulk)}$	$\delta^{18}O_{GHW(calc)}$*	$\delta^{18}O_{H2O(calc)}$**
G2-21/21B	-2.6	-2.5	+4.3	-0.4	-9.9	-13.4

G3-7/7B	-3.4	-3.2	+1.0	-2.0	-8.0	-11.5
G3-10/10B	-4.5	-4.2	-2.0	-3.5	-6.4	-9.9
G5a-14/14B	+0.3	+0.2	+2.8	-0.2	-6.2	-9.7

Values are given in ‰. *Gypsum hydration water (GHW) $\delta^{18}O$ was calculated using the measurements of bulk gypsum $\delta^{18}O$ and $\delta^{18}O$ of the sulfate part; **Mother water $\delta^{18}O$ was calculated from the $\delta^{18}O_{GHW}$ using the fractionation factor given by Gázquez et al. (2017).

The obtained results from the test for $\delta^{34}S$ were almost the same, with very small differences which fall within the measurement error (Table 1). As oxygen isotopes were also measured for the test samples - we could calculate indirectly the $\delta^{18}O$ value of the gypsum hydration water (GHW) from the measurements of bulk gypsum $\delta^{18}O$ and sulfate part $\delta^{18}O$ using the following equation: $\delta^{18}O_{gypsum(bulk)} = Y * \delta^{18}O_{SO4} + (1-Y) * \delta^{18}O_{GHW}$, where Y is the ratio of sulfate oxygen to total gypsum oxygen, and 1-Y is the ratio of hydration water oxygen to total gypsum oxygen. From the GHW $\delta^{18}O$ value, we can calculate the $\delta^{18}O$ value of the mother water from which the gypsum precipitated, using the fractionation factor ($\alpha^{18}O_{gypsum\text{-}water} = 1.0035$) given by Gázquez et al. (2017), which was shown to be very insensitive to temperature. Although these values (Table 1) are estimations (with error larger than the measurement error) and haven't been confirmed by direct measurements, they are similar to the measured $\delta^{18}O$ values from Melnica Spring (-9.7 to -10 ‰, unpublished data) and $\delta^{18}O$ values obtained from fluid inclusions in the calcite crust from the speleogenetic phase preceding the SAS (-12 ‰; Dublyansky, 2013 pers. comm.).

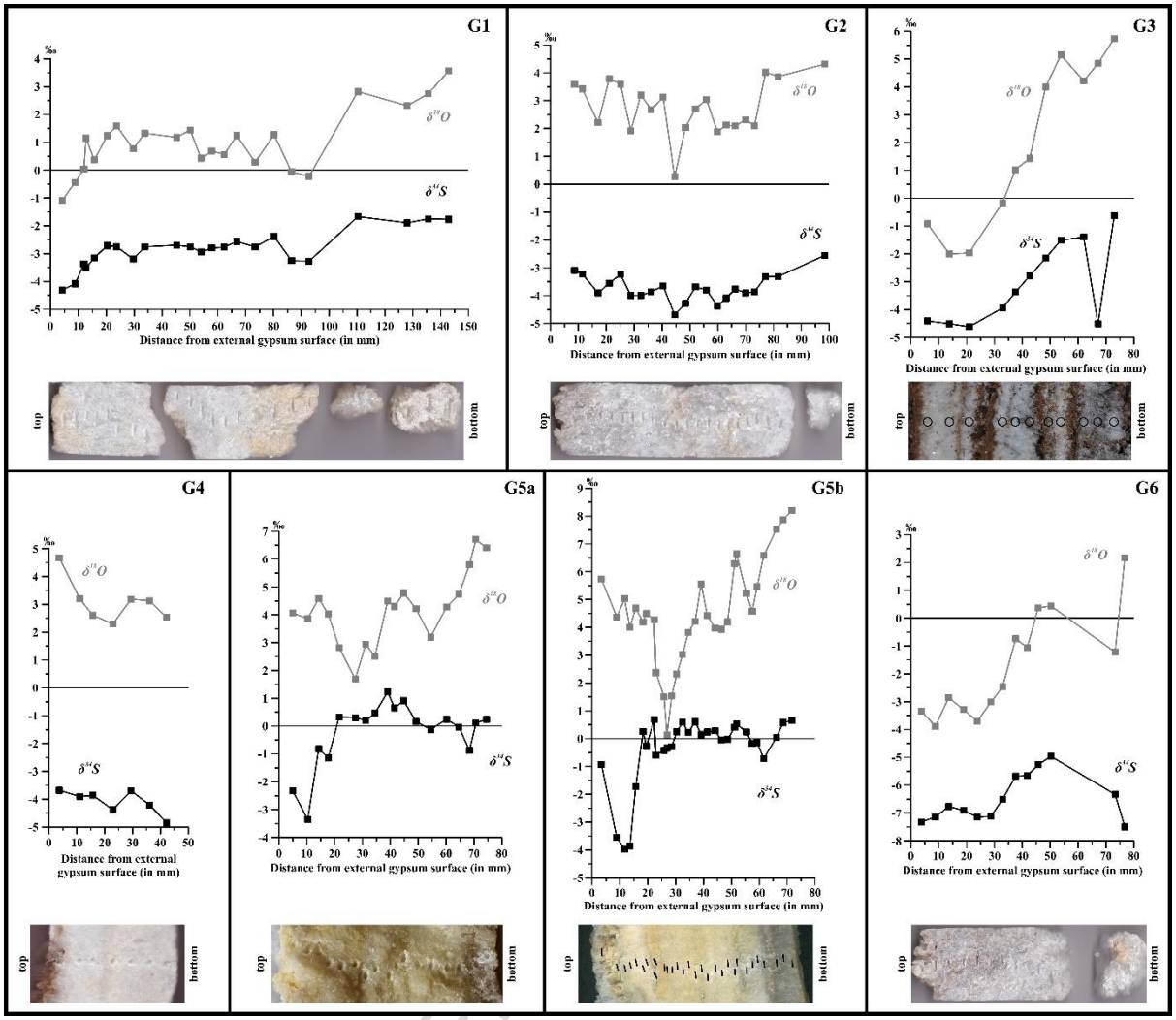

Fig. 4. View of the sampled gypsum deposits with graphs of $\delta^{18}O$ and $\delta^{34}S$ variation along the sampling lines. This figure is available in color online at https://www.journals.elsevier.com/geomorphology.

5. Results and discussion

5.1. Distribution of $\delta^{18}O$ and $\delta^{34}S$ values

The measured sub-samples show a wide range of values for both $\delta^{18}O$ and $\delta^{34}S$, with sulfur values ranging from -7.5 ‰ to +0.7 ‰ and oxygen values ranging from -3.9 ‰ to +8.2 ‰ (Table 2). The range of $\delta^{34}S$ values is much wider than the previously reported values of -2.1 ‰ and -2.2 ‰ (Temovski et al., 2013).

Table 2. General statistics for the measured sample datasets

Data set	Isotopes	Min	Max	Mean	SD	Range	N	R	R^2	p
		‰								
All	$\delta^{34}S$	-7.5 (-7.3)	+0.7	-2.9 (-2.8)	2.1	8.2 (8.0)	105 (100)	0.726 (0.780)	0.527 (0.608)	<0.001
	$\delta^{18}O$	-3.9	+8.2	+2.3 (+2.2)	2.6	12.1				
G1	$\delta^{34}S$	-4.3	-1.7	-2.8	0.7	2.6	23	0.903	0.815	<0.001
	$\delta^{18}O$	-1.1	+3.6	+1.0	1.1	4.6				
G2	$\delta^{34}S$	-4.7	-2.6	-3.7	0.5	2.1	21	0.886	0.785	<0.001
	$\delta^{18}O$	+0.3	+4.3	+2.8	1.0	4.0				
G3	$\delta^{34}S$	-4.6	-0.6	-3.1 (-2.9)	1.5	4.0	11 (10)	0.774 (0.985)	0.599 (0.970)	0.005 (<0.001)
	$\delta^{18}O$	-2.0	+5.7	+1.9 (+1.7)	3.0 (2.9)	7.7				
G4	$\delta^{34}S$	-4.8	-3.7	-4.1	0.4	1.2	7	0.621	0.386	0.137
	$\delta^{18}O$	2.3	+4.7	+3.1	0.8	2.4				
G5b	$\delta^{34}S$	-4.0 (-1.7)	+0.7	-0.4 (+0.0)	1.3 (0.6)	4.7 (2.4)	30 (27)	0.104 (0.225)	0.011 (0.051)	0.585 (0.259)
	$\delta^{18}O$	+0.1	+8.2	+4.5	1.9 (2.0)	8.1				
G6	$\delta^{34}S$	-7.5 (-7.3)	-5.0	-6.5 (-6.4)	0.8	2.5 (2.4)	13 (12)	0.484 (0.971)	0.234 (0.943)	0.093 (<0.001)
	$\delta^{18}O$	-3.9	+2.2 (+0.4)	-1.7 (-2.1)	1.9 (1.6)	6.1 (4.3)				
Group A	$\delta^{34}S$	-7.5 (-7.3)	-2.6	-4.7 (-4.6)	1.4 (1.3)	4.9 (4.8)	41 (40)	0.903 (0.973)	0.815 (0.947)	<0.001
	$\delta^{18}O$	-3.9	+4.7	+1.4	2.5	8.6				
Group B	$\delta^{34}S$	-4.6	-0.6	-2.9	1.0	4.0	34 (33)	0.751 (0.934)	0.564 (0.872)	<0.001
	$\delta^{18}O$	-2.0	+5.7	+1.3 (+1.2)	1.9 (1.8)	7.7				

Values calculated without outliers (sub-samples G3-2, G5b-27, G5b-28, G5b-29, G6-13), if different, are given in parenthesis. For G5, values from subset G5b were used for the statistics, as profile line G5b has better sampling resolution than G5a.

When plotted, the $\delta^{18}O$-$\delta^{34}S$ values show two end-member groups: G5 having the highest values and G6 having the lowest values for both $\delta^{18}O$ and $\delta^{34}S$ (Fig. 5). The others can be placed in two intermediate groups, with samples G2 and G4 having a trend of $\delta^{18}O$ and $\delta^{34}S$ values with smaller range and slightly lower $\delta^{34}S$ values than G1 and G3. Five values appear

as outliers in the samples (subsets), three in G5b and one in each of G3 and G6. The similar trends and values of $\delta^{18}O$ and $\delta^{34}S$ from the two sub-sampling profiles in G5 show that the outliers (two in G5a and three in G5b) are not an artefact of the measurements, and can be considered as outliers to the relationship of $\delta^{18}O$ and $\delta^{34}S$ values in the subset. The range of the $\delta^{18}O$ values is almost double that of the $\delta^{34}S$ values in all of the samples, except for G5 where it is more than three times larger.

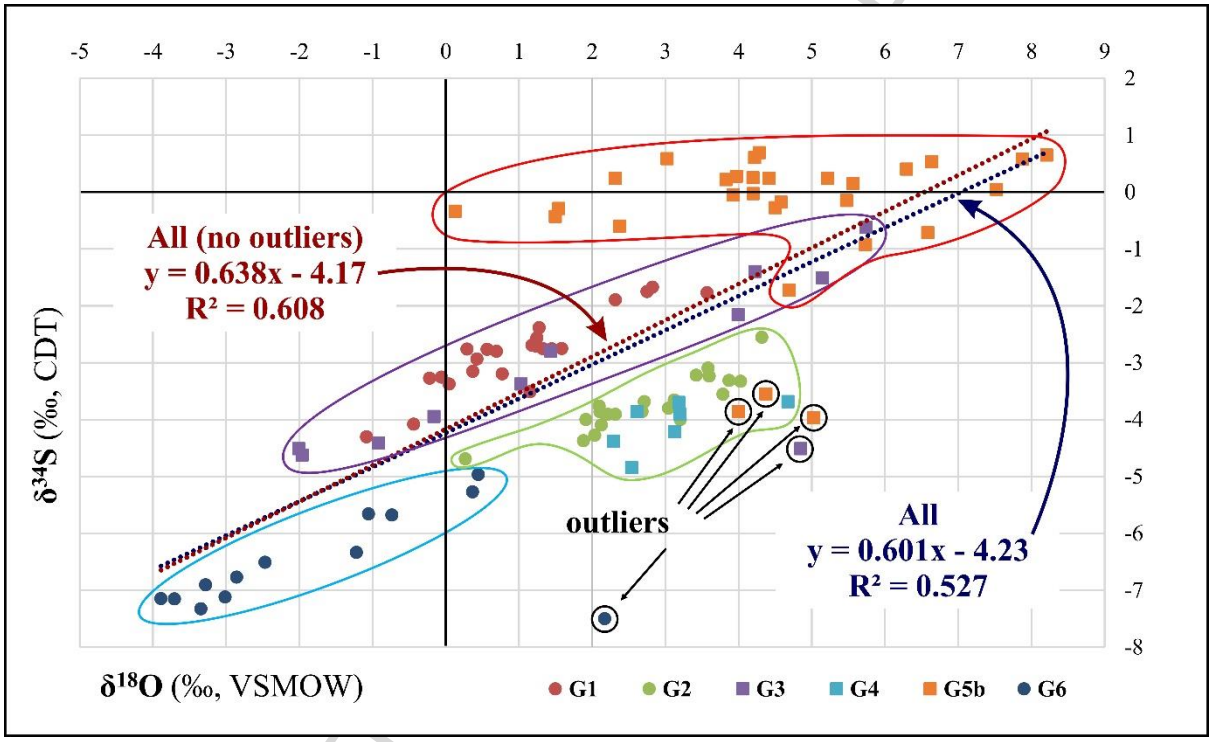

Fig. 5. Scatter plot of co-variation of $\delta^{34}S$ with $\delta^{18}O$ values with linear regression lines of all data (N=105) and data after removal of five subset outliers (N=100). This figure is available in color online at https://www.journals.elsevier.com/geomorphology.

Both $\delta^{18}O$ and $\delta^{34}S$ values show variations along the sampled profiles (Fig. 4). In samples G1, G2, G5 and G6 there is a slight trend of increase in both values with greater distance from the sample surface. This trend can be valid also for G4, which is a piece from a collapsed (and overturned) gypsum crust, thus its current position should be reversed. As the

speleogenetic gypsum forms by replacement of the carbonate rock, the deposits should be progressively younger towards the gypsum-bedrock interface, and this trend of increase in values might reflect change of conditions as the replacement of carbonate bedrock progressed. G3 also has this trend, but this sample has a stratigraphy of alternating gypsum and silty-sandy layers, which could indicate either their precipitation below the water table, or more likely re-deposition of a number of collapsed replacement crusts, and thus it is not comparable to the other replacement crust samples.

5.2. Co-variation of the $\delta^{18}O$ and $\delta^{34}S$ values

There is a strong positive correlation between the $\delta^{18}O$ and the $\delta^{34}S$ values for the whole dataset (N=105) with R=0.726 at $p<0.001$ (Table 2). These values are slightly better if the five outliers in G3, G5b, and G6 are removed, showing that 61 % of the variation in the $\delta^{34}S$ values can be explained by their linear relationship with the $\delta^{18}O$ values ($R^2=0.608$), with even higher percentages for four of the six subsets (Table 2). The only sample that shows no correlation between the $\delta^{18}O$ and the $\delta^{34}S$ values is G5 (both subsets), although this sample morphologically appears similar to the other sampled replacement crusts.

The remaining samples have values that have two distinct linear trends, with G2, G4 and G6 as Group A, and G1 and G3 as Group B (Fig. 6; Table 2). Their values (without the two outliers) show almost perfect correlation with 87 % to 95 % of the variation in the $\delta^{34}S$ values explained by their linear relationship with the $\delta^{18}O$ values. Both groups have also almost identical slope, indicating that for every 1 ‰ increase in the $\delta^{18}O$ value, there is a ~0.5 ‰ increase in the $\delta^{34}S$ value. Group B has a higher intercept than Group A which shows that there is a general change of +1.85 ‰ in the $\delta^{34}S$ value. This change in the $\delta^{34}S$ must have occurred prior to the H_2S oxidation, as the oxygen is obtained during the oxidation, and

indicates systemic change of the H_2S $\delta^{34}S$ value which might be due to changes in the source area (H_2S production). Another possibility is that the change occurred within the cave system, due to increase in the fractionation of sulfur during H_2S degassing, as $\delta^{34}S$ of the $H_2S_{(g)}$ becomes more positive with the increase of pH in the water (Baune and Böttcher, 2010).

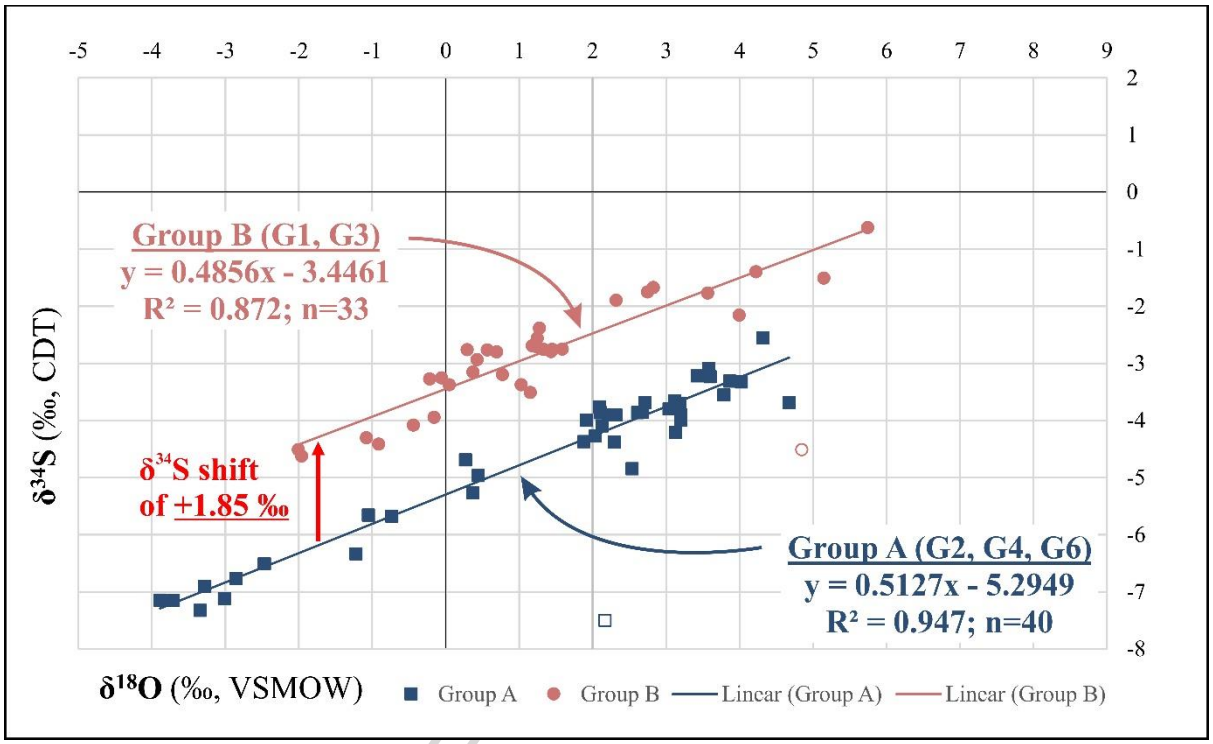

Fig. 6. Scatter plot of co-variation of $\delta^{34}S$ with $\delta^{18}O$ values with linear regression lines for data grouped in two groups: A (samples G2, G4 and G6) and B (samples G1 and G3). Outliers (not used for the regression lines) are shown with open symbols. This figure is available in color online at https://www.journals.elsevier.com/geomorphology.

5.3. The source of oxygen

As discussed before, the $\delta^{18}O$ values depend on the contribution and isotope values of the two possible sources (H_2O and O_2), as well as their oxygen enrichment factors with sulfate. Since we do not know the exact enrichment factors, we cannot quantitatively determine the

contribution of H_2O or O_2 oxygen, but we can still qualitatively discriminate between their contributions, as atmospheric O_2 and groundwater have distinctively different $\delta^{18}O$ values (Van Stempvoort and Krouse, 1994; Onac et al., 2011). The $\delta^{18}O$ of the atmospheric oxygen is +23.8 ‰ (Horibe et al., 1973), and for the water we can use the values from the Melnica thermal spring located below the cave, which has $\delta^{18}O$ of -10 ‰ (unpublished data), and is similar to the $\delta^{18}O$ values indirectly calculated from gypsum hydration water (Table 1), although slight variations are to be expected due to effects of evaporation-condensation in the cave.

The $\delta^{18}O$ values in Provalata Cave gypsum deposits range from -3.9 ‰ to +8.2 ‰, but if corrected for the oxygen fractionation during gypsum precipitation (min. +2 ‰, max. +3.6 ‰), the estimated $\delta^{18}O$ values of the sulfate prior to gypsum precipitation will be negatively shifted and have wider possible range, between -7.5 ‰ and +6.2 ‰. All of them fall within the theoretical boundaries and can be explained by a combination of various fractions of oxygen derived from H_2O or O_2 and different oxygen enrichment factors (Fig. 7).

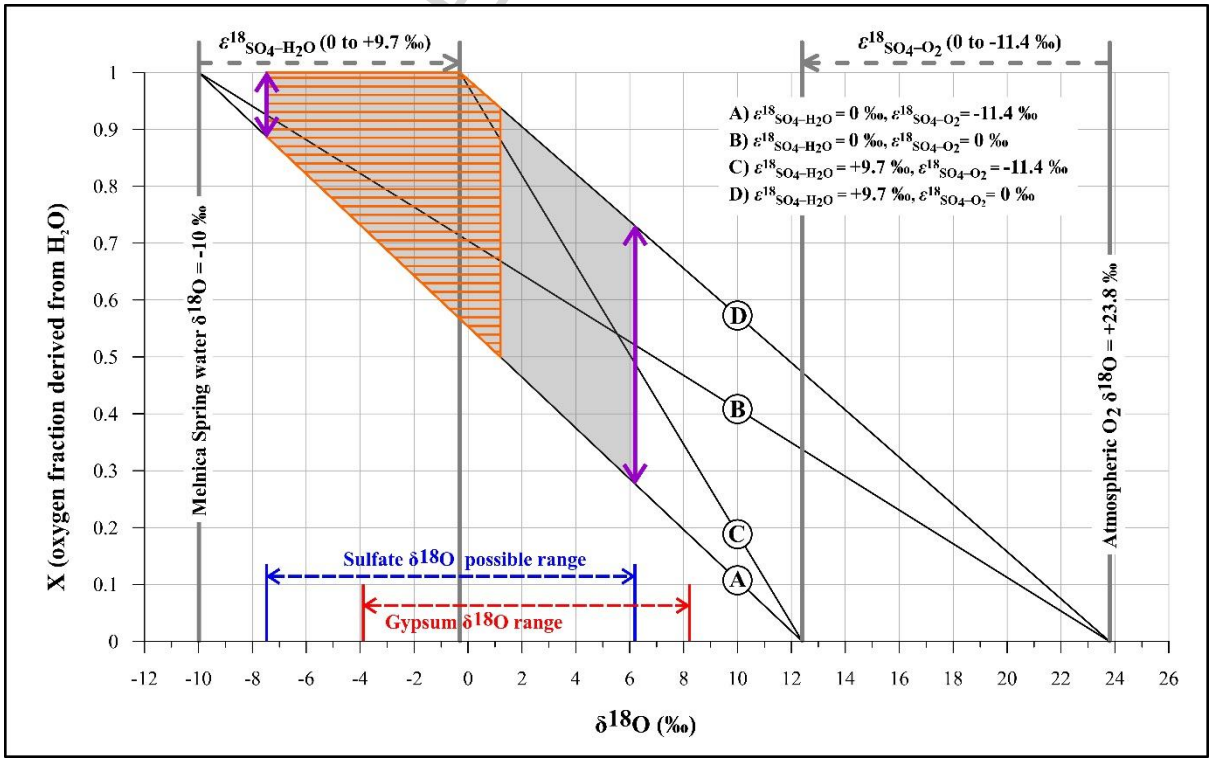

Fig. 7. Modeling the range of Provalata Cave gypsum $\delta^{18}O$ values using different oxygen source contributions (H_2O or O_2) and oxygen enrichment factors with sulfate. Shaded area – range of possible combinations between oxygen sources and enrichment factors to produce the sulfate $\delta^{18}O$ values. The range of sulfate $\delta^{18}O$ was inferred from Provalata Cave gypsum $\delta^{18}O$ values, corrected for the fractionation during gypsum precipitation. Hatched area – range of sulfate $\delta^{18}O$ values for which more than half of the oxygen was derived from H_2O. Thick arrow-headed lines – possible ranges of oxygen fraction derived from H_2O to produce the lowest (-7.49 ‰) and highest (+6.20 ‰) possible sulfate $\delta^{18}O$ values. This figure is available in color online at https://www.journals.elsevier.com/geomorphology.

To produce the highest estimated sulfate $\delta^{18}O$ values (+6.2 ‰), at various combinations of oxygen enrichment factors, the possible H_2O oxygen contribution can range between 28 % and 73 %, while for the lowest $\delta^{18}O$ values this range is between 89 % and 100 % (Fig. 7). If we consider lower values for the water $\delta^{18}O$ (-13.4 ‰; as estimated from the gypsum hydration water), then H_2O oxygen contribution will be slightly smaller with 24-64 % for the highest and 77-100 % for the lowest sulfate $\delta^{18}O$ values. Using $\delta^{18}O_{H2O}$ of -10 ‰, we can estimate that more than half of the oxygen was derived from H_2O for sulfate $\delta^{18}O$ values lower than +1.2 ‰, and lower than -0.5 ‰ for $\delta^{18}O_{H2O}$ of -13.4 ‰. This indicates that H_2O is the main contributor of oxygen for the H_2S oxidation, with more positive values indicative of oxidation under more oxic conditions.

The source of O_2 can be either from the cave atmosphere due to aeration of the cave, or brought in by seepage of O_2-rich vadose waters. In Provalata Cave, the connection of the cave passages with the surface (allowing vadose percolation) is very poor. Except below the cave entrance (a collapse structure), vadose percolation can be seen only in a few more

locations where gypsum deposits have been partially or completely dissolved, and some flowstone speleothems have been deposited (Temovski et al., 2013). Most of the cave passages lack any indication of vadose percolation of water. When the SAS was active, the connection with the surface was surely much more subdued. Nevertheless, some connections might have existed, enough to provide O_2 by air circulation that would then dissolve in the condensation water droplets on the cave walls.

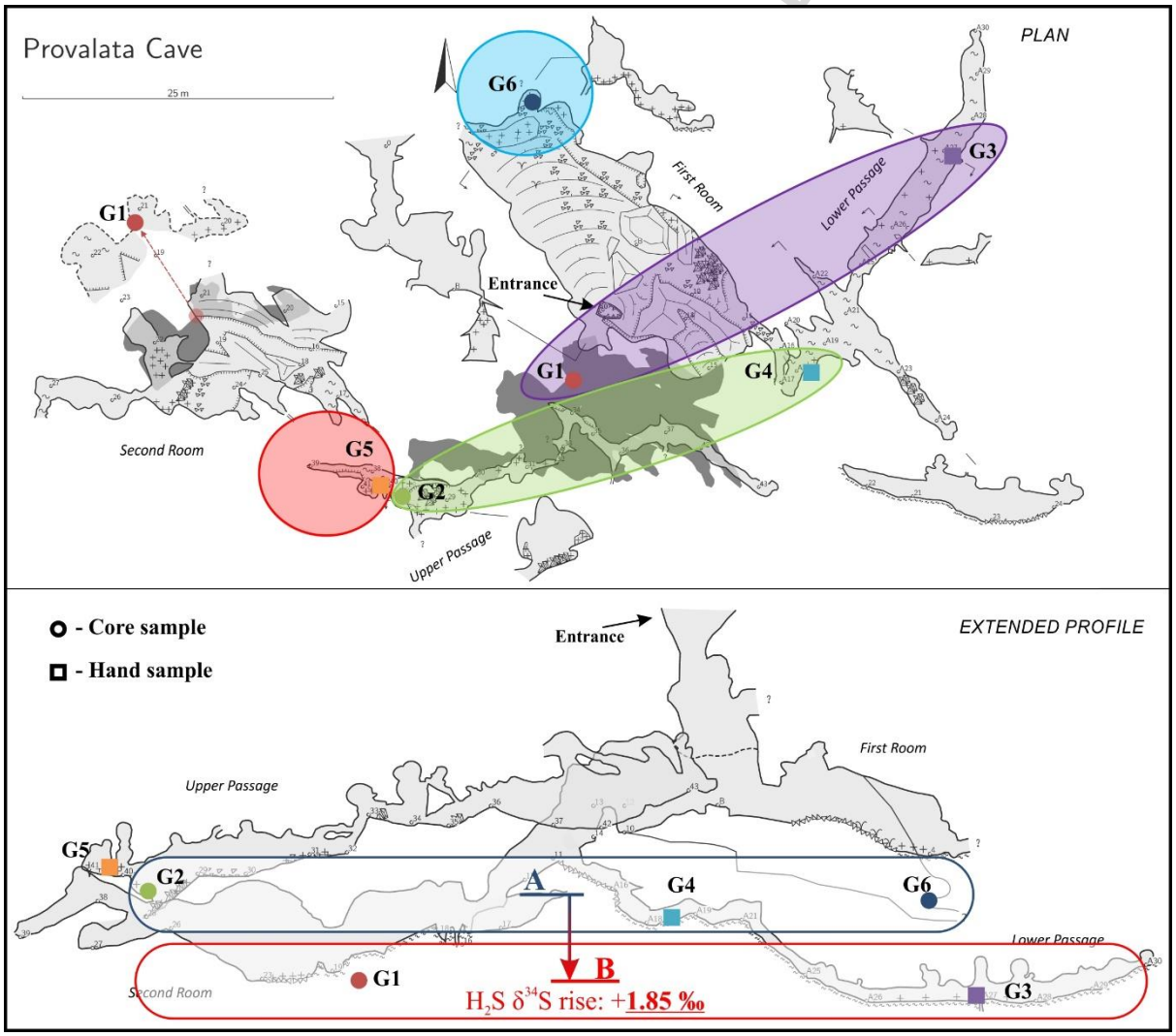

Fig. 8. Spatial distribution of $\delta^{18}O$ and $\delta^{34}S$ values in Provalata Cave gypsum deposits. This figure is available in color online at https://www.journals.elsevier.com/geomorphology.

5.4. Spatial distribution of the $\delta^{18}O$ and $\delta^{34}S$ values

In terms of spatial distribution (Fig. 8), the lowest values of both $\delta^{18}O$ and $\delta^{34}S$ (sample G6) are found in the northern part of the cave (First Room), while the highest are from sample G5, located in the southwestern part of the cave (Upper Passage). The spatial distribution of the other samples is consistent with their distribution on the $\delta^{18}O$-$\delta^{34}S$ plot (Fig. 5), with G2-G4 located slightly to the south from G1-G3. In both of these groups one sample is from the eastern part of the cave (Lower Passage) and one from the western/southwestern part, but G2-G4 are located at slightly lower depth than G1-G3. The lower values of the northern samples indicates formation under more anoxic conditions than the southern ones. Their development might have been closer to the water table, as the flow of water was northward towards Buturica Valley. This is also comparable to the distribution of condensation-corrosion morphologies, which are more abundant in the southern part of the cave, especially in the Upper Passage (Temovski et al., 2013). The +1.85 ‰ shift in the $\delta^{34}S$ values seen between Groups A (G2, G4, G6) and B (G1, G3) relates also to their positions at different depths within the cave. Although we do not know the difference in age of formation for these deposits, the evolution of the SAS in the cave should have progressed downward due to lowering of the water table, with the incision of the nearby valley (Temovski et al., 2013), thus the deeper parts should be younger. Considering this, the positive shift in the $\delta^{34}S$ values with depth can be also connected to the temporal evolution of the SAS system.

Sample G5 is located very close to G2, but has much more positive values for both $\delta^{18}O$ and $\delta^{34}S$, although showing no correlation between them. Also, its location depth is similar to the ones from Group A but its high $\delta^{34}S$ values (together with the highest $\delta^{18}O$ values) fit better

with the ones from Group B, and these gypsum deposits might be younger in age than those of Group A, despite their position.

5.5. Control on the co-variation of $\delta^{18}O$ and $\delta^{34}S$ during H_2S oxidation

The oxygen in the sulfate is obtained during the oxidation of H_2S, thus the strong correlation of oxygen and sulfur isotope values in Provalata gypsum deposits indicates that both oxygen and sulfur isotopes were concurrently affected during the oxidation process, which in sulfuric acid caves is most likely to occur through microbial pathways (Hose et al., 2000; Engel et al., 2004; Jones et al., 2015).

Another possible explanation for the strong co-variation between the $\delta^{18}O$ and $\delta^{34}S$ values can be that they are produced by mixing between two sulfate sources with distinctively different isotope signatures: one with high $\delta^{18}O$ and $\delta^{34}S$ values and the other with low $\delta^{18}O$ and $\delta^{34}S$ values. However, gypsum replacement crusts are formed in sub-aerial settings (Galdenzi and Maruoka, 2003; Palmer, 2013), with H_2S oxidizing to H_2SO_4 in condensation water droplets on cave walls, dissolving the carbonate rock and precipitating gypsum as crusts. In such settings, it is unlikely to have sulfate with highly contrasting $\delta^{18}O$ and $\delta^{34}S$ values produced concurrently during H_2S oxidation at very close locations. Oxidation of pyrite from the carbonate bedrock as a possible second sulfate source in addition to the one produced by H_2S oxidation is excluded here, as pyrite is very rare in the calcite marble bedrock. Also in most of the sampled locations (e.g. G2, G4, G5, G6) sulfuric acid dissolution has not (or has only partly) reached the marble bedrock, with gypsum crusts replacing mostly thick calcite crusts.

Gypsum precipitation which follows the oxidation of H_2S, fractionates also both oxygen and sulfur isotopes. Van Driessche et al. (2016) found that during gypsum precipitation, oxygen

fractionation shows stronger temperature dependence than sulfur fractionation (sulfur having lower values at higher temperatures). Nevertheless, at temperatures below 40 °C, and for different saturation indexes, they found only small variations in the fractionation of sulfur and oxygen. Thus, while the values of $\delta^{18}O$ and $\delta^{34}S$ are affected (increased for a certain fractionation factor) during gypsum precipitation, it is unlikely to have large variations in fractionation factors, and the correlation between $\delta^{18}O$ and $\delta^{34}S$ reflects the linear relationship obtained during oxidation.

As pointed out, the variation in the oxygen values might be due to variation in the O_2 contribution, which was most likely derived from the cave air. Thus cave aeration might have been an important factor controlling the isotope composition of the cave sulfates. Higher aeration would have provided higher O_2 concentration, allowing for a higher contribution of O_2 during oxidation, and producing sulfate with higher $\delta^{18}O$ values. During chemolithotrophic sulfide oxidation there is an inverse isotope effect on sulfur (up to +8 ‰; Zerkle et al., 2016). In the Frassasi Cave it was found that fractionation higher than +4 ‰ only occurs at lower H_2S and/or higher O_2 concentrations (Zerkle et al., 2016). This can explain the positive correlation of $\delta^{18}O$ and $\delta^{34}S$ values in the produced sulfate, with higher $\delta^{18}O$ and $\delta^{34}S$ values indicating oxidation under more oxic conditions, and lower values indicating oxidation under more anoxic conditions. If so, then cave aeration affecting the supply of O_2 in the cave atmosphere (with infiltration of vadose O_2-rich water considered as minor during the SAS in Provalata Cave), and probably also the diffusion of H_2S out of the cave, can be the main control on the variation of the sulfur and oxygen isotopes in the Provalata Cave speleogenetic gypsum.

Small variations in the oxygen and sulfur isotopes that do not follow the correlation between $\delta^{18}O$ and $\delta^{34}S$ might be due to additional effects such as small variations in local conditions

during oxidation (e.g. contribution of abiotic oxidation) or gypsum precipitation (e.g. variations in the fractionation factors).

The very small variation of $\delta^{34}S$ and large variation of $\delta^{18}O$ in G5 cannot be explained by the same combined effect of fractionation of sulfur and oxygen during microbial oxidation and concentrations of H_2S and O_2. Their positive $\delta^{34}S$ values indicate microbial oxidation under lower H_2S/O_2 conditions. Their $\delta^{34}S$ values and the highest $\delta^{18}O$ values (> +5 ‰) fit within the trend of Group B, but there is a large negative shift in the oxygen values indicating larger contribution of water oxygen, which might indicate also lower concentration of O_2 (more anoxic conditions).

In addition to the environmental control, another possible control for the linear correlation between the $\delta^{18}O$ and $\delta^{34}S$ values can be the combined isotope fractionation during multi-step microbial metabolism. Different biochemical mechanisms during chemolithotrophic sulfide oxidation can produce different important sulfur intermediates (e.g. S^0 or SO_3), although these mechanisms and their associated isotope effects are still not well characterized (Zerkle et al., 2016). This may also explain the lack of correlation seen in G5, with different organisms having different oxidation pathways with different isotope fractionations connected to different sulfur intermediates.

6. Conclusions

Application of both oxygen and sulfur stable isotopes in the study of SAS gypsum deposits can be illustrative on the conditions under which sulfuric acid speleogenesis operated, as well as on the evolution of the SAS system.

Our results show strong positive linear correlation between the $\delta^{18}O$ and $\delta^{34}S$ values with a ~0.5 ‰ increase in the $\delta^{34}S$ for every 1 ‰ increase in the $\delta^{18}O$. The $\delta^{18}O$ values indicate that

most of the oxygen during H_2S oxidation was derived from H_2O, with more positive values indicating oxidation under more oxic conditions, attributed to higher cave aeration. As the oxygen is obtained during the oxidation of H_2S, the strong correlation indicates that both oxygen and sulfur isotopes were concurrently affected during the oxidation process. These effects are considered to be either due to environmental control (concentrations of H_2S and O_2) or due to combined isotope fractionation during multi-step microbial oxidation, also affected by the environmental conditions. Two parallel trends of linear correlation of $\delta^{18}O$ and $\delta^{34}S$ values show a shift of +1.85 ‰ in the $\delta^{34}S$ prior to oxidation, indicating an evolutionary change of $\delta^{34}S$ in the SAS system, either as a result of isotopic changes in the source area (during production of H_2S) or due to higher fractionation during degassing of H_2S as a result of change in water chemistry.

The wide range of $\delta^{18}O$ and $\delta^{34}S$ values in Provalata Cave gypsum deposits, and their spatial distribution, shows that the number of studied samples and their location can be an important factor in the understanding of sulfuric acid speleogenesis using stable isotopes. With only few studies reporting both sulfur and oxygen isotope composition of SAS gypsum deposits, more detailed studies are needed from sulfuric acid caves on the $\delta^{18}O$ and $\delta^{34}S$ distribution within their gypsum deposits. Better understanding of the isotope fractionation of both oxygen and sulfur during multi-step microbial oxidation of H_2S in active sulfuric acid caves is also needed to better constrain the environmental controls on the $\delta^{18}O$ and $\delta^{34}S$ values in the speleogenetic gypsum deposits.

Acknowledgement

We would like to thank Darko Nedanoski and Jovan Todorovski from SK Zlatovrv – Prilep for assistance during sampling. We are also thankful to Jo De Waele and Simon Bottrell for

their constructive reviews that improved the manuscript, and to Editor-in-Chief Andrew Plater for careful editing of the final version. This research was carried out as part of the MTA Postdoctoral Fellowship Programme, No. PP-030/2015, and was partly supported by the European Union and the State of Hungary, co-financed by the European Regional Development Fund in the project of GINOP-2.3.2-15-2016-00009 'ICER'.

References

Audra, P., Hobléa, F., Bigot, J.-Y., Nobécourt, J.-C., 2007. The role of condensation–corrosion in thermal speleogenesis: study of a hypogenic sulfidic cave in Aix-les-Bains, France. Acta Carsologica 36, 185–194. http://dx.doi.org/10.3986/ac.v36i2.186

Baune, C., Böttcher, M.E., 2010. Experimental investigation of sulphur isotope partitioning during outgassing of hydrogen sulphide from diluted aqueous solutions and seawater. Isotopes in Environmental and Health Studies 46(4), 444-453. https://doi.org/10.1080/10256016.2010.536230

Bottrell, S.H., 1991. Sulphur isotope evidence for the origin of cave evaporites at Ogof y Daren Cilau, south Wales. Mineralogical Magazine 55, 209–210.

Bottrell, S.H., Crowley, S., Self, C., 2001. Invasion of a karst aquifer by hydrothermal fluids: evidence from stable isotopic compositions of cave mineralization. Geofluids 1, 103-121. http://dx.doi.org/10.1046/j.1468-8123.2001.00008.x

De Waele, J., Audra, P., Madonia, G., Vattano, M., Plan, L., D'Angeli, I.M., Bigot, J.-Y., Nobécourt, J.-C., 2016. Sulfuric acid speleogenesis (SAS) close to the water table: Examples from southern France, Austria, and Sicily. Geomorphology 253, 452-467. https://doi.org/10.1016/j.geomorph.2015.10.019

Egemeier, S.J., 1981. Cavern development by thermal waters. NSS Bull. 43, 31–51.

Engel, A.S., Stern, L.A., Bennet, P.C., 2004. Microbial contributions to cave formation: new insights into sulfuric acid speleogenesis. Geology 32, 369–372. https://doi.org/10.1130/G20288.1

Fry, B., Ruf, W., Gest, H., Hayes, J.M., 1988. Sulfur isotope effects associated with oxidation of sulfide by O_2 in aqueous solution. Chemical Geology 73, 205–210. https://doi.org/10.1016/0168-9622(88)90001-2

Galdenzi, S., Cocchioni, M., Morichetti, L., Amici, V., Scuri, S., 2008. Sulfidic ground-water chemistry in the Frasassi Caves, Italy. Journal of Cave and Karst Studies 70 (2), 94–107.

Galdenzi, S., Maruoka, T., 2003. Gypsum deposits in the Frasassi caves, Central Italy. Journal of Cave and Karst Studies 65, 111–125.

Gázquez, F., Evans, N.P., Hodell, D.A. 2017. Precise and accurate isotope fractionation factors ($\alpha^{17}O$, $\alpha^{17}O$ and αD) for water and $CaSO_4 \cdot 2H_2O$ (gypsum). Geochimica et Cosmochimica Acta 198, 259-270. http://dx.doi.org/10.1016/j.gca.2016.11.001

Grasby, S.E., van Everdingen, R.O., Bednarski, J., Lepitzki, D.A.W., 2003. Travertine mounds of the Cave and Basin National Historic Site, Banff National Park. Canadian Journal of Earth Sciences 40, 1501–1513. https://doi.org/10.1139/e03-058

Hill, C.A., 1987. Geology of Carlsbad cavern and other caves in the Guadalupe Mountains, New Mexico and Texas. New Mex. Bur. Min. Mineral Resour. Mem. 117, 1–150.

Horibe, Y., Shigehara, K., Takakuwa, Y., 1973. Isotope separation factors of carbon dioxide-water system and isotopic composition of atmospheric oxygen. Journal of Geophysical Research 78, 2625–2629. http://dx.doi.org/10.1029/JC078i015p02625

Hose, L.D., Palmer, A.N., Palmer, M.V., Northup, D.E., Boston, P.J., DuChene, H.R., 2000. Microbiology and geochemistry in a hydrogen sulphide rich karst environment. Chemical Geology 169, 399–423. https://doi.org/10.1016/S0009-2541(00)00217-5

Jones, D.S., Polerecky, L., Galdenzi, S., Dempsey, B.A., Macalady, J.L., 2015. Fate of sulfide in the Frasassi cave system and implications for sulfuric acid speleogenesis. Chemical Geology 410, 21–27. https://doi.org/10.1016/j.chemgeo.2015.06.002

Lloyd, R.M., 1968. Oxygen isotope behavior in the sulfate-water system. Journal of Geophysical Research 73, 6099–6110. http://dx.doi.org/10.1029/JB073i018p06099

Mansor, M., Harouaka, K., Macalady, J.L., Fantle, M.S., 2016. Oxidative sulfur isotope fractionation on sulfidic cave walls. 2016 Goldschmidt Conference Abstracts, p. 1964.

Onac, B.P., Wynn, J.G., Sumrall, J.B., 2011. Tracing the sources of cave sulfates: a unique case from Cerna Valley, Romania. Chemical Geology 288, 105–114. https://doi.org/10.1016/j.chemgeo.2011.07.006

Palmer, A.N., 1991. Origin and morphology of limestone caves. Geological Society of America Bulletin, 103(1), 1-21. https://doi.org/10.1130/0016-7606(1991)103%3C0001:OAMOLC%3E2.3.CO;2

Palmer, A.N., 2013. Sulfuric acid caves: Morphology and Evolution. In: Frumkin, A., Shroder, J. (Eds.), Treatise on Geomorphology. Elsevier, 241–257.

Piccini, L., De Waele, J., Galli, E., Polyak, V.J., 2015. Sulphuric acid speleogenesis and landscape evolution: Montecchio cave, Albegna river valley (Southern Tuscany, Italy). Geomorphology 229, 134-143. http://dx.doi.org/10.1016/j.geomorph.2014.10.006

Plan, L., Tschegg, C., De Waele, J., Spötl, C., 2012. Corrosion morphology and cave wall alteration in an Alpine sulfuric acid cave (Kraushöhle, Austria). Geomorphology 169-170, 45-54. https://doi.org/10.1016/j.geomorph.2012.04.006

Raab, M., Spiro, B., 1991. Sulfur isotopic variations during seawater evaporation with fractional crystallization. Chemical Geology: Isotope Geoscience Section 86, 323-333. https://doi.org/10.1016/0168-9622(91)90014-N

Spötl, C., Mattey, D., 2012. Scientific drilling of speleothems – a technical note. International Journal of Speleology 41, 29-34. http://dx.doi.org/10.5038/1827-806X.41.1.4

Temovski, M., Audra, P., Mihevc, A., Spangenberg, J., Polyak, V., McIntosh, W., Bigot, J.-Y., 2013. Hypogenic origin of Provalata Cave, Republic of Macedonia: a distinct case of successive thermal carbonic and sulfuric acid speleogenesis. International Journal of Speleology 42(3), 235–264. http://dx.doi.org/10.5038/1827-806X.42.3.7

Thode, H.G., Monster, J., 1965. Sulfur-isotope geochemistry of petroleum, evaporites, and ancient seas. American Association of Petroleum Geologists Memoir 4 (1965), 367-377.

Van Driessche, A.E.S., Canals, A., Ossorio, M., Reyes, R.C., García-Ruiz, J.M., 2016. Unraveling the sulfate sources of (giant) gypsum crystals using gypsum isotope fractionation factors. Journal of Geology 124, 235-245. https://doi.org/10.1086/684832

Van Everdingen, R.O., Shakur, M.A., Krouse, H.R., 1985. Role of corrosion by H_2SO_4 fallout in cave development in a travertine deposit - evidence from sulfur and oxygen isotopes. Chemical Geology 49, 205–211. https://doi.org/10.1016/0009-2541(85)90156-1

Van Stempvoort, D.R., Krouse, H.R., 1994. Controls of sulfate $\delta^{18}O$: a general model and application to specific environments. In: Alpers, C., Blowes, D. (Eds.), Environmental Geochemistry of Sulfide Oxidation. American Chemical Society Symposium Series, 550, 446–480.

Wynn, J.G., Sumrall, J.B., Onac, B.P., 2010. Sulfur isotopic composition and the source of dissolved sulfur species in thermo-mineral springs of the Cerna Valley, Romania. Chemical Geology 271, 31–43. https://doi.org/10.1016/j.chemgeo.2009.12.009

Zerkle, A.L., Jones, D.S., Farquhar, J., Macalady J.L., 2016. Sulfur isotope values in the sulfidic Frasassi cave system, central Italy: a case study of a chemolithotrophic S-based ecosystem Geochimica et Cosmochimica Acta 173, 373-386. https://doi.org/10.1016/j.gca.2015.10.028

LIST OF FIGURES

Fig. 1. Location and geological setting of Provalata Cave. Nerezi Formation is composed of clastic sediments and Vitačevo and Mariovo Formations of volcanoclastic sediments.

Fig. 2. Location and type of gypsum samples collected from Provalata Cave.

Fig. 3. Photos of sampling locations within the cave: A – Slightly detached gypsum replacement crust in a small side passage in Second Room (G1); B – Detached gypsum replacement crust close to the wall of a dome-like enlargement at the junction of passages in the Upper Passage (G2); C – Gypsum layers alternating with thin sandy layers on the foothill

of the wall in the Lower Passage (G3); D – Gypsum crust covering the floor in the upper parts of the Lower Passage (G4); E - Slightly detached gypsum crust which was covering calcite crust in a small dead-end part of the Upper Passage (G5); F – Gypsum replacement crust below a cupola carved in both calcite crust and bedrock in the northern end of the First Room (G6). Photos by M. Temovski.

Fig. 4. View of the sampled gypsum deposits with graphs of $\delta^{18}O$ and $\delta^{34}S$ variation along the sampling lines.

Fig. 5. Scatter plot of co-variation of $\delta^{34}S$ with $\delta^{18}O$ values with linear regression lines of all data (N=105) and data after removal of five subset outliers (N=100).

Fig. 6. Scatter plot of co-variation of $\delta^{34}S$ with $\delta^{18}O$ values with linear regression lines for data grouped in two groups: A (samples G2, G4 and G6) and B (samples G1 and G3). Outliers (not used for the regression lines) are shown with open symbols.

Fig. 7. Modeling the range of Provalata Cave gypsum $\delta^{18}O$ values using different oxygen source contributions (H_2O or O_2) and oxygen enrichment factors with sulfate. Shaded area – range of possible combinations between oxygen sources and enrichment factors to produce the sulfate $\delta^{18}O$ values. The range of sulfate $\delta^{18}O$ was inferred from Provalata Cave gypsum $\delta^{18}O$ values, corrected for the fractionation during gypsum precipitation. Hatched area – range of sulfate $\delta^{18}O$ values for which more than half of the oxygen was derived from H_2O. Thick arrow-headed lines – possible ranges of oxygen fraction derived from H_2O to produce the lowest (-7.49 ‰) and highest (+6.20 ‰) possible sulfate $\delta^{18}O$ values.

Fig. 8. Spatial distribution of $\delta^{18}O$ and $\delta^{34}S$ values in Provalata Cave gypsum deposits.

LIST OF TABLES

Table 1. Results of test measurements for control of isotope changes during conversion of gypsum to barium sulfate.

Values are given in ‰. *Gypsum hydration water (GHW) $\delta^{18}O$ was calculated using the measurements of bulk gypsum $\delta^{18}O$ and $\delta^{18}O$ of the sulfate part; **Mother water $\delta^{18}O$ was calculated from the $\delta^{18}O_{GHW}$ using the fractionation factor given by Gázquez et al. (2017).

Table 2. General statistics for the measured sample datasets

Values calculated without outliers (sub-samples G3-2, G5b-27, G5b-28, G5b-29, G6-13), if different, are given in parenthesis. For G5, values from subset G5b were used for the statistics, as profile line G5b has better sampling resolution than G5a.

Highlights

- Use of both $\delta^{18}O$ and $\delta^{34}S$ in the study of gypsum deposits from a sulfuric acid cave
- Positive correlation between $\delta^{18}O$ and $\delta^{34}S$ due to both oxygen and sulfur isotopes being concurrently affected during H_2S oxidation
- Evolution of the sulfur stable isotopes in the H_2S of the sulfuric acid speleogenesis